



Article

# Grid-Scale Regional Risk Assessment of Potentially Toxic Metals Using Multi-Source Data

Mulin Chen <sup>1,2</sup>, Hongyan Cai <sup>1,\*</sup> , Li Wang <sup>3</sup> and Mei Lei <sup>4</sup> 

<sup>1</sup> State Key Laboratory of Resources and Environmental Information System, Institute of Geographic Sciences and Natural Resources Research, Chinese Academy of Sciences, Beijing 100101, China; chenml.19b@igsnr.ac.cn

<sup>2</sup> University of Chinese Academy of Sciences, Beijing 100049, China

<sup>3</sup> Key Laboratory of Land Surface Pattern and Simulation, Institute of Geographical Sciences and Natural Resources Research, Chinese Academy of Sciences, Beijing 100101, China; wangli@igsnr.ac.cn

<sup>4</sup> Center for Environmental Remediation, Institute of Geographic Sciences and Natural Resources Research, Chinese Academy of Sciences, Beijing 100101, China; leim@igsnr.ac.cn

\* Correspondence: caihy@igsnr.ac.cn

**Abstract:** Understanding the risks posed by potentially toxic metals (PTMs) in large regions is important for environmental management. However, regional risk assessment that relies on traditional field sampling or administrative statistical data is labor-intensive, time-consuming, and coarse. Internet data, remote sensing data, and multi-source data, have the advantage of high speed of collection, and can, thereby, overcome time lag challenges and traditional evaluation inefficiencies, although, to date, they are rarely applied. To evaluate their effectiveness, the current study used multi-source data to conduct a 1 km scale assessment of PTMs in Yunnan Province, China. In addition, a novel model to simulate potentially hazardous areas, based on atmospheric deposition, was also proposed. Assessments reveal that risk areas are mainly distributed in the east, which is consistent with the distribution of mineral resources in the province. Approximately 3.6% of the cropland and 1.4% of the sensitive population are threatened. The risk areas were verified against those reported by the government and the existing literature. The verification exercise confirmed the reliability of multi-source data, which are cost-effective, efficient, and generalizable for assessing pollution risks in large areas, particularly when there is little to no site-specific contamination information.

**Keywords:** fine-scale polluted risk assessment; internet data mining; cropland vulnerability; human health; heavy metals contamination; management strategies



**Citation:** Chen, M.; Cai, H.; Wang, L.; Lei, M. Grid-Scale Regional Risk Assessment of Potentially Toxic Metals Using Multi-Source Data. *ISPRS Int. J. Geo-Inf.* **2022**, *11*, 427. <https://doi.org/10.3390/ijgi11080427>

Academic Editors: Godwin Yeboah and Wolfgang Kainz

Received: 22 May 2022

Accepted: 25 July 2022

Published: 28 July 2022

**Publisher's Note:** MDPI stays neutral with regard to jurisdictional claims in published maps and institutional affiliations.



**Copyright:** © 2022 by the authors. Licensee MDPI, Basel, Switzerland. This article is an open access article distributed under the terms and conditions of the Creative Commons Attribution (CC BY) license (<https://creativecommons.org/licenses/by/4.0/>).

## 1. Introduction

Potentially toxic metals (PTMs) contamination resulting from anthropogenic activities, particularly industrial activities related to metalliferous mining, smelting, and refining, poses a serious threat to the environment and human health [1,2]. In this sense, precisely assessing the risk state is a prerequisite for environmental management and risk reduction.

Contamination risk assessments conducted at local to regional scales can be divided into two major groups: site-specific assessments [3,4] and regional assessments [5,6]. Site-specific assessments produce absolute evaluations of risk for one or more contaminated sites through sampling and laboratory analyses [7]; they typically involve, for example, carcinogenic and non-carcinogenic risk indices [7,8]. In contrast, regional scale risk assessments are concerned with a large expanse of land or territory, usually an administrative area [9]. As they aim to evaluate the relative importance of risks by ranking them magnitude-wise for the entire region [10], they are often referred to as relative evaluation methods [11].

Implementing a risk prevention management plan is usually a regional-scale exercise [12], and regional assessments are more feasible for developing comprehensive control strategies than site-specific assessments [10]. Furthermore, regional assessments aiming to

identify and screen for potential contaminated sites requiring further investigation [13–15] generally constitute the critical first mapping step toward the overall identification, assessment, and management of contaminated sites [16].

However, regional investigations remain sparse [17]. The primary impediment may be the difficulty in obtaining data. For regions where data are unavailable, administrative statistical data or a meta-analysis is usually used for assessment [18–20]. For example, a review of the published literature shows that provinces located in southern and southwestern China are most contaminated by cadmium (Cd), hydrargyrum (Hg), lead (Pb), and arsenic (As) [21–23]. These studies, however, were usually performed at a coarse scale, e.g., the administrative unit scale [22,23]. The fate and transport of pollutants and their dynamics depend on the spatiotemporal framework considered [10], and knowledge gaps with respect to detailed risks limit their support for decision-making. Assessments at fine scales (e.g., a gridded scale) are more effective, not only for describing risks in detail, but also for aiding the precise mapping of high-risk areas.

For regions where field sampling data are available, assessments are generally conducted using the sources–pathways–receptors (SPR) concept [10,11,14]. Risks are described by sources (i.e., contaminated sites), pathways (i.e., water, air, and direct contact), and receptors (i.e., environmental or human health) in terms of scores [10]. However, field surveys over a large region are costly, laborious, and time-consuming. For example, China's first soil pollution census cost USD 125 million and took 9 years, from 2005 to 2013 [24]. More importantly, the survey data are usually confidential, making the search for new data sources imperative for developing regional risk assessment frameworks.

With the rapid development of 3S (geographic information system, GIS; global position system, GPS; and remote sensing, RS), location-based services (LBS) and internet data mining technology, internet data, remote sensing images, and reanalysis data, among others, multi-source data rendered their superiority for the rapid detection of pollution sources and the determination of receptor sensitivity [25,26]. Specifically, these data have the advantage of a high collection speed [27,28], and can, thereby, overcome time lag challenges and traditional evaluation inefficiencies. However, the application of multi-source data in regional risk assessment is rare, and multi-source data for promoting regional risk assessment are largely unknown.

The objective of this study was to apply multi-source data for PTMs regional risk assessment on a gridded scale, and evaluate the effectiveness of such data for risk identification and assessment. Yunnan Province, a metal-mining center in China, served as a case study. The study here will improve our ability to assess, classify, identify, and map contamination risks in large regions, and thereby better support decision-making.

## 2. Materials and Methods

### 2.1. Study Area

Yunnan is a typical province in the mountainous border area of southwest China (31°42'–39°35' N and 105°29'–111°15' E). It consists of 13 cities and 165 counties, covering nearly 390 thousand km<sup>2</sup>. The dominant wind direction in the province is SSE–S–SSW, and the average wind speed ranges from 2 to 6 m/s (Figure 1). Average annual precipitation is generally high in the southwest, and exceeds 2000 mm [29]. In 2020, the population of children (≤14 years old), adults, and the elderly (≥60 years old) was 9.23 million (19.57%), 30.93 million (65.52%), and 7.03 million (14.91%), respectively.

The province is rich in zinc (Zn), Cd, Pb, and tin (Sn) mine resources [30]. By 2010, 142 types of mineral deposits had been discovered in the province, accounting for 83% of those identified nationally [31]. Intensive metal mining and processing activities have seriously damaged environmental and public health. According to previous studies, Yunnan and two other provinces are the most polluted provinces in China due to Cd, copper (Cu), Pb, and Zn contamination [23,32]. In addition, a high incidence of lung disease as an occupational hazard was observed in Yunnan's miners, due to exposure to As and radon [33].

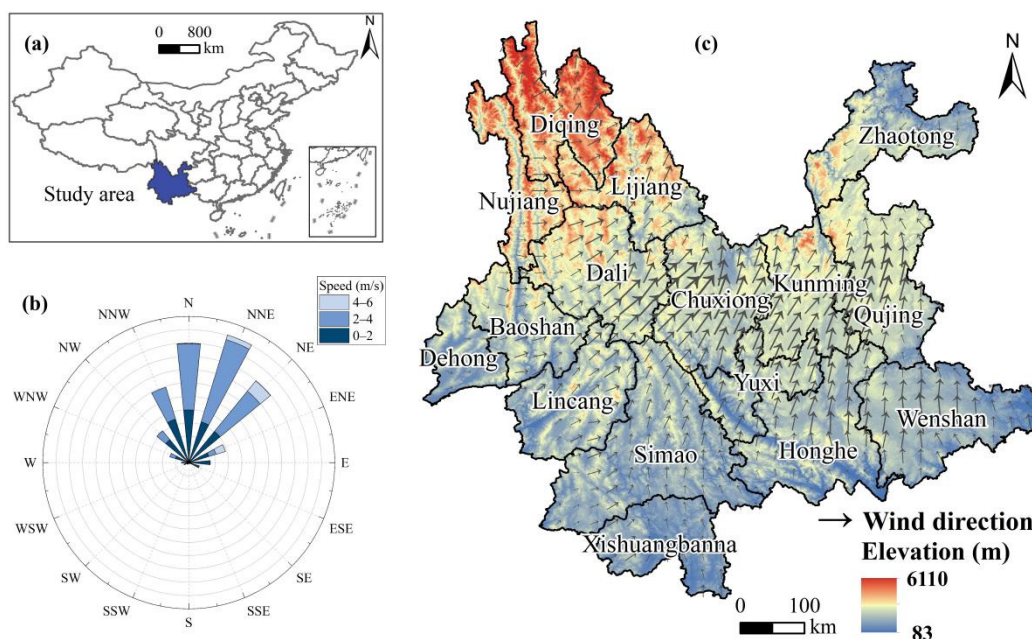


**Figure 1.** Study area. (a) Location of Yunnan in China; (b) predominant wind directions and speeds (m/s); (c) spatial distributions of elevation and wind speed magnitude and direction.

2.2. Materials

2.2.1. Pollution Sources Data

Here, pollution sources refer to metal-related industrial plants. Using internet data mining technology, the industrial plants were crawled from major internet platforms in China, namely TianYanCha (<https://www.tianyancha.com/>, accessed on 12 February 2019) and the Green Network Environment Data Center (GNEDC) (<http://www.lvwang.org.cn/>, accessed on 12 February 2019). Via collection, cleaning, geographic location transcoding, and coordinate correction, details of 1710 industrial plants were obtained. Data for each plant included name, location, duration of operation, industrial type, and an industrial index (II). The last parameter describes the adverse effects of pollution-related enterprises, by evaluating the illegal storage, disposal, and discharge activities of a given industrial plant [34]. Among the 1710 plants, 1354 (79.1%) were in operation in 2020, and the remaining ones (18.5%) were closed (Table 1).

**Table 1.** Description of the data used in this study.

	Data	Resolution	Time Span	Data Collection or Generation
Sources	Metal-related industrial plants that registered online	-	1982–2020	Collected from the internet platforms using an internet data mining technology
	Soil texture	1 km	-	Downloaded from the Harmonized World Soil Database
Pathways	Precipitation	1 km	2006–2020 Yearly data	Interpolated from station records using the cubic spline interpolation method, with elevation as an independent covariate in the ANUSPLIN software
	Wind speed	0.1°	1990–2020 Monthly data	Generated by ERA5 weather forecasting models
	Relief amplitude	1 km	-	Calculated based on DEM images using the window analysis method and the focal statistics function in ArcGIS [35]
	NPP	1 km	2000–2020 Yearly data	Downloaded from MODIS remote sensing images
Receptors	Population densities of children and the elderly	1 km	2020	Simulated by a spatialization technique

### 2.2.2. Pathways Data

According to the ‘Plot in Production Plant Risk Screening and Risk Classification Technical Regulations (Try Out)’ of China [36], the pathways data mainly consisted of soil texture, multi-year average precipitation, multi-year average wind speed, and relief amplitude (Table 1).

### 2.2.3. Receptors Data

For the receptors data, according to the ‘Technical guidelines for risk assessment of soil contamination of land for construction (HJ 25.3–2019)’ [37], cropland and humans are treated as the main receptors. The elderly population and children were selected as the sensitive populations, due to their relatively poor immunity [21], and the density of the sensitive population was estimated by using a spatialization technique [38]. Details are shown in the Supplementary Material (Figure S1).

The productivity of cultivated land served as the indicator of cropland vulnerability. It was quantified by the MODIS net primary productivity (NPP) products (MOD17A3H), because NPP is strongly correlated with agricultural productivity [39].

### 2.3. Methodology

The methodology comprised three steps, which are outlined in Figure 2. The first step was to collect regional data for the risk assessment, as mentioned above. A detailed description of the other two steps is provided in the following paragraphs.

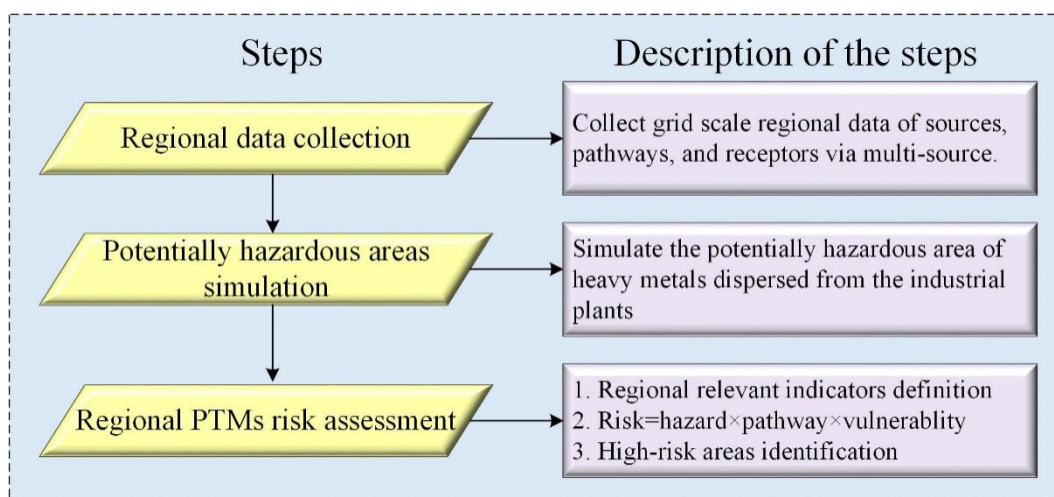


**Figure 2.** Framework of the proposed regional risk assessment of potentially toxic metals (PTMs).

#### 2.3.1. Potentially Hazardous Area Simulation

Industrial activities typically threaten the surrounding areas [40]. Accordingly, we defined an area around each industrial plant as the potentially hazardous area (PHA). Any area within the PHA could face risks, whereas areas lying outside the PHA were considered risk-free. In the previous literature, a buffer area of a radius  $d$  was used to denote the PHA [10,11], e.g., 6.5 km [41]. However, industrial plants vary greatly in terms of their production scale, operation duration, production technology, and geo-environmental locations, and adopting a uniform PHA for all industrial plants is, thus, not justified. Instead, an adaptive PHA simulation is needed for accurate assessments [10].

To simulate the PHA, industrial types, operation time, precipitation, and wind were considered, referring to the ‘Technical Provisions for the Detailed Investigation of Soil Pollution in Agricultural Land’ [42]. The effect of wind on PTMs dispersal is directional [43,44]. Prevailing winds strongly influence the delivery of PTMs [45–47], and tend to form an elliptical pollution footprint in surrounding areas downwind from the pollutant source [48,49]. Thus, the area impacted by wind was presumed to be an ellipse [50,51], whereas a circle

was assumed for the area impacted by factors other than wind, because their dispersion effect tends to be directionless. On this basis, the conceptual model used for the PHA simulation has the following steps:

1. Simulating the elliptical area impacted by wind. The location of a given industrial plant constitutes the vertex of the ellipse, and the direction of its major axis is consistent with that of the prevailing wind. The lengths of the major and minor axes are shown in Table 2. Each monthly wind condition generates an ellipse (Figure 3a);

**Table 2.** Dispersal distances from metal mining, smelting, and refining industries [42].

Metal Mining Industry (Base Distance is 1.0 km)			
Adjustment Factors		Adjusted Distance (km)	
Duration of operation (years)	<15	0.0	
	≥15	+0.5	
Multi-year mean precipitation (mm)	<400	+1.0	
	400–800	0.0	
	>800	−0.5	
Dispersal distance by wind			
Monthly wind speed (m/s)		Minor axis	Major axis
	<3	1.0 km	1.5 km
	3–5	1.5 km	2.0 km
	5–7	2.0 km	2.5 km
	>7	3.0 km	3.5 km
Metal Smelting and Refining Industry (Base Distance is 1.5 km)			
Adjustment factors		Adjusted distance (km)	
Duration of operation (years)	<5	0.0	
	5–15	+1.0	
	> 15	+2.0	
Multi-year mean precipitation (mm)	<400	+0.5	
	400–800	0.0	
	>800	−0.5	
Dispersal distance by wind			
Monthly wind speed (m/s)		Minor axis	Major axis
	<2	2.0 km	3.0 km
	2–4	1.5 km	2.5 km
	>4	1.0 km	2.0 km

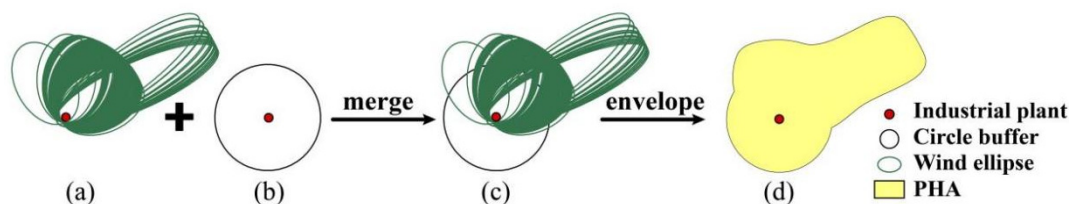


**Figure 3.** Conceptual model of the potentially hazardous area simulation. (a) Ellipses are generated according to monthly wind conditions. (b) Circle buffer of a given industrial plant. (c) The circle buffer and the ellipses are merged into a new feature. (d) The potentially hazardous area (PHA) is generated by enveloping the merged feature.

2. Simulating the circular area impacted by other factors. A circle buffer is generated based on industrial types, operation time, and multi-year mean precipitation of the location. The radius of the circle is equal to the sum of the base distance and adjusted distances (Figure 3b, Table 2);
3. Merging the circle buffer with all the ellipses (Figure 3c);
4. Defining the smoothed enveloping surface extracted from the merged feature as the final PHA (Figure 3d).

### 2.3.2. Regional Risk Assessment of Potentially Toxic Metals (PTMs)

In contrast to the coarse assessments in the previous literature, risk was assessed at a 1 km scale in the current study. The choice of the 1 km scale originated from the ‘Technical Provisions for the Detailed Investigation of Soil Pollution in Agricultural Land’ [42]. As indicated by the guideline, areas impacted by metal mining, smelting, and refining industries are generally located 1 to 5 km from industrial plants. With this in mind, we chose a 1 km scale for our assessment to properly capture the minimum impacted area. Based on the SPR concept, the risk was scored by the hazard posed by the industrial plants, the dispersal of the pathway, and the vulnerability of the receptor.

The hazard score ( $H$ ) was estimated by three indicators using Equations (1) and (2). To obtain detailed spatial information on hazard, the  $H$  scores were interpolated to a 1 km spatial resolution raster for the extent of the PHA by using the inverse distance-weighted (IDW) method [52]. Subsequently, the  $H$  scores were normalized according to Table 3.

$$H_n = DT_n + II_n + K_n \quad (1)$$

$$DT_n = \begin{cases} 2020 - T_s & \text{operative industrial plant} \\ \frac{T_e - T_s}{2020 - T_e} & \text{closed industrial plant} \end{cases} \quad (2)$$

where  $DT$ ,  $II$ ,  $K$ ,  $T_e$ , and  $T_s$  are the duration time, industrial index, kernel density, and the start and the end operative time points of the  $n$ th industrial plant, respectively;  $DT$ ,  $II$ , and  $K$  were normalized to 0–1 before calculating  $H$ .

**Table 3.** Scores used for indicators normalization in the case study.

	Indicators	Classes	Scores	Classes	Scores	Classes	Scores
Sources	Hazard ( $H$ )	$\geq 0.5$	5	[0.15,0.5)	3	<0.15	1
	Soil texture ( $ST$ )	Sand	5	Silt loam	3	Clay loam	1
Pathways	Precipitation ( $P$ ) (mm/yr)	$\geq 1000$	5	[400,1000)	3	<400	1
	Wind speed ( $WS$ ) (m/s)	<2	5	[2,4)	3	$\geq 4$	1
	Relief amplitude ( $RA$ ) (m)	$\geq 1500$	5	[1000,1500)	3	<1000	1
Receptors	Yield of cropland	High yields	5	Moderate yields	3	Low yields	1
	Sensitive population density (per/km <sup>2</sup> )	$\geq 3000$	5	[1000,3000)	3	<1000	1

The pathway dispersal score ( $P$ ) was obtained using Equation (3). The four assessment indicators were normalized prior to the calculations (Table 3). The normalization of soil texture and precipitation was based on the ‘Technical Provisions for the Detailed Investigation of Soil Pollution in Agricultural land’ [42], and the normalization of relief amplitude was based on the terrain division standard [53].

$$P_i = \frac{1}{4}(ST_i + p_i + WS_i + RA_i) \quad (3)$$

The receptor vulnerability scores ( $V$ ) were expressed as the productivity of cropland and the population density. The type of cropland was determined based on the NPP according to the method of Shi et al. [54].

The respective risk score ( $R$ ) posed to cropland and sensitive populations of the  $i$ th grid cell was characterized by Equation (4), and the total overall risk was summed by the two assessed risk scores (Equation (5)):

$$R_i = H_i \times P_i \times V_i \quad (4)$$

$$R_{\text{Overall}} = R_{\text{cropland}} + R_{\text{population}} \quad (5)$$

where  $R_{\text{overall}}$ ,  $R_{\text{cropland}}$ , and  $R_{\text{population}}$  represent the assessed overall, cropland, and sensitive population risks, respectively.

Subsequently, the risk at the county level was determined by summing the risk at the gridded level within the administrative area. The risk scores were then divided into three classes (low, moderate, and high) according to the natural breakpoint method [11]. The high-class areas were designated as high-risk areas.

### 3. Results

#### 3.1. Spatial Distribution of the Industrial Plants

The industrial plants were grouped into the following categories: metal-mining (948) and metal-smelting and refining (762) industries, which mainly include Cu, Zn, and Sn tailing, as well as smelting plants. The industries were established between 1982 and 2020; further information on the duration, industrial index, and hazard scores is presented in Table S1. Spatially, the plants are concentrated in the eastern province, especially in Honghe City, followed by the cities of Kunming, Qujing, and Baoshan (Figure 4). The high abundance of resource-oriented industrial plants is consistent with the distributions of mineral resources in the province [55].

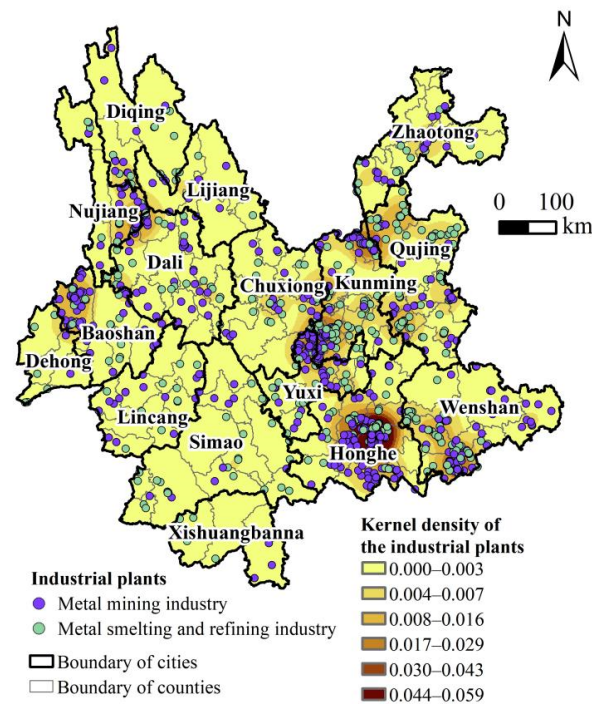


**Figure 4.** Spatial distribution of the industrial plants.

#### 3.2. Risk Assessment Results

##### 3.2.1. Risk Assessment at the 1-km Scale

The three components of the SPR concept include hazard, pathway, and vulnerability scores (Figure 5). Generally, the hazard score map corresponds to the distribution of the industrial plants (Figure 5a). Higher values are mainly distributed in the east of the province, such as in the cities of Honghe and Wenshan. The distribution difference of the pathway scores in the province is mainly determined by soil texture and relief amplitude. The high-score areas are located in the cities of Honghe, Baoshan, and Kunming (Figure 5b). Regarding vulnerability, the high-score areas of sensitive population vulnerability are about 21.1%, whereas the number of croplands is about 8.0% (Figure 5c).

The 1 km scale risk maps reveal that risk areas are mainly distributed in the east, with the high-risk areas primarily concentrated in Honghe City, which contains central and north-eastern Gejiu County (Figure 6). Statistically, approximately 3.6% of cropland (2952 km<sup>2</sup>) is found to be threatened, where 278 km<sup>2</sup> of cropland faces a high risk (Figure 7a). Regarding

population assessment, the sensitive population of 680,000 people, facing a greater risk, accounts for 1.4% of the total population (Figure 7b).

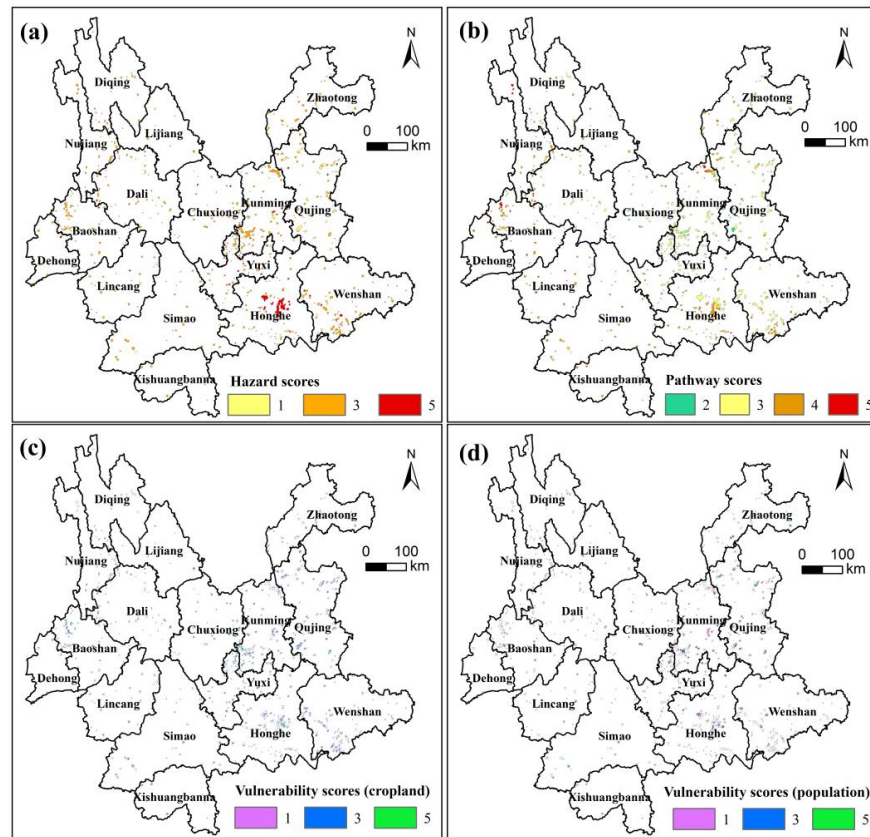


**Figure 5.** The 1 km scale risk assessment for (a) hazard scores, (b) pathway scores, and vulnerability of cropland (c), and population (d).

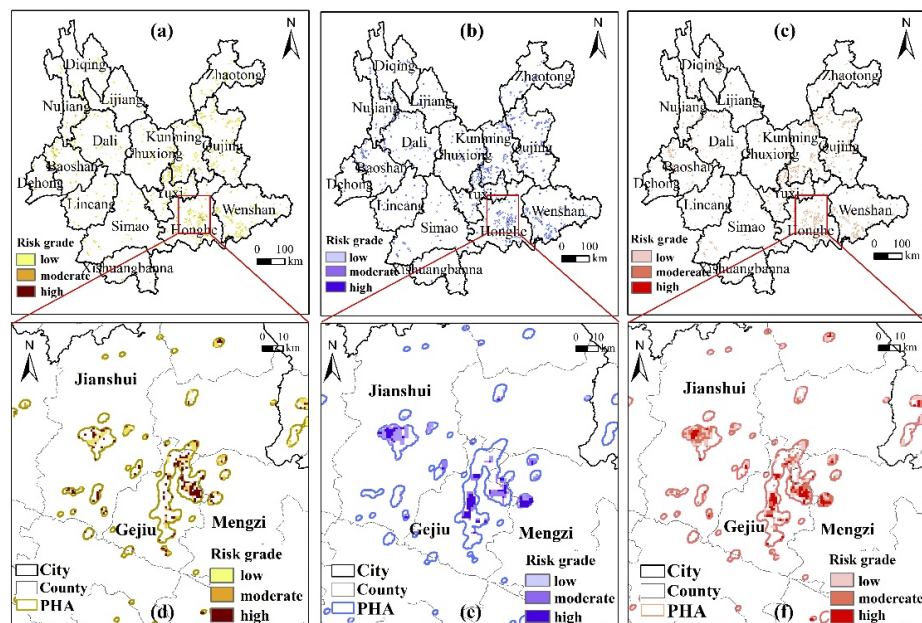


**Figure 6.** The 1 km scale risk assessment for (a) cropland, (b) sensitive populations, and (c) overall risk in Yunnan. In Honghe City, the risk assessment is shown for (d) cropland, (e) sensitive populations, and (f) overall risk. PHA is the potentially hazardous area simulation.



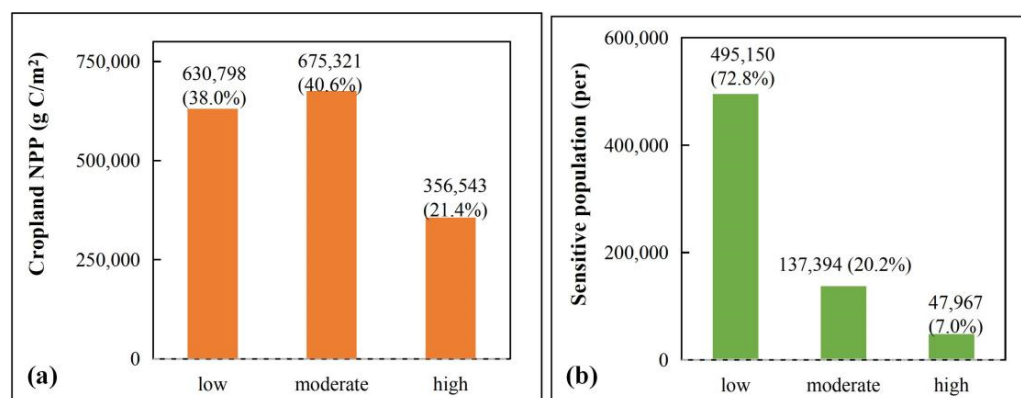


**Figure 7.** The 1 km scale risk assessment results. (a) Total amount and proportion of cropland NPP affected by different risk grades and (b) number and proportion of people in the sensitive population affected by different risk grades.

### 3.2.2. Risk Assessment at the County Scale

For cropland risk assessment, the counties of Gejiu and Tengchong are identified as high-risk areas (Figure 8a). Tengchong incurs the maximal threat to cropland, as it has both the highest cropland vulnerability score (433) and the largest exposed cropland area (137 km<sup>2</sup>) (Table S2, Figure 8d).

For the sensitive population risk assessment, two high-risk regions (Gejiu and Jianshui) are distinguished (Figure 8b). The life expectancy there is 6 and 2 years lower than the provincial average in 2000 and 2010, respectively [56]. The high-risk score of Jianshui is mainly attributed to its large area of residential settlements (113 km<sup>2</sup>) exposed to industrial plants (Table S2, Figure 8e).

In the overall risk assessment, four high-risk regions and eight moderate-risk regions are identified (Figure 8c). Gejiu is threatened most significantly because it has the highest hazard score (2325) and the highest dispersal pathway score (1745) (Table S2, Figure 8f). This county is known as the “Tin Capital” for its world-class tin–polymetallic deposits [57], and is home to 345 plants related to tin mining and smelting, nearly one third of the province’s total. Consequently, its natural environment is largely affected by intensive mining activities. This county had the highest male lung cancer mortality in a nationwide survey conducted in 1973 [58], mainly due to occupational As exposure and smoking [59]. Although great efforts were made in cancer diagnosis and treatment, lung cancer remains the leading cause of cancer-related mortality in Gejiu [57].

### 3.3. Verification

To verify the accuracy, we validated the three components and the assessed counties at risk. The hazard scores were compared to heavy metals concentrations, which were obtained by the meta-analysis. In total, 37 cases studies were collected from Google Scholar, Web of Science, and China National Knowledge Infrastructure. Given that the current study focuses on industrial plants, we further targeted publications whose study areas were also industrial plants. In addition, to maintain a consistent period, we screened the literature published between 2015 and 2020. Finally, a total of 16 cases studies were reviewed (Table S3), and 932 soil samples were analyzed.

The seven main heavy metals in Yunnan Province, namely, As, Cd, Cr, Cu, Hg, Pb, and Zn, were selected for the verification [60,61]. On the basis of heavy metals concentrations, the Nemerow integrated pollution index (NIPI) was calculated, and divided into four levels: safe (NIPI < 1), slight pollution (1 < NIPI < 2), moderate pollution (2 < NIPI < 3), and heavy pollution (NIPI > 3) [62]. The results show that the counties of Xianggelila, Lanping, Dongchuan, Huize, Longling, and Gejiu are heavily polluted (Figure 9h). Similarly, the hazard scores of Xianggelila, Lanping, Dongchuan, Huize, and Gejiu are significantly higher than those of the other counties (Figure 9i). This leads us to infer that the hazard

scores estimated using online industrial plant data can reflect the pollution state of the environment, to some extent.

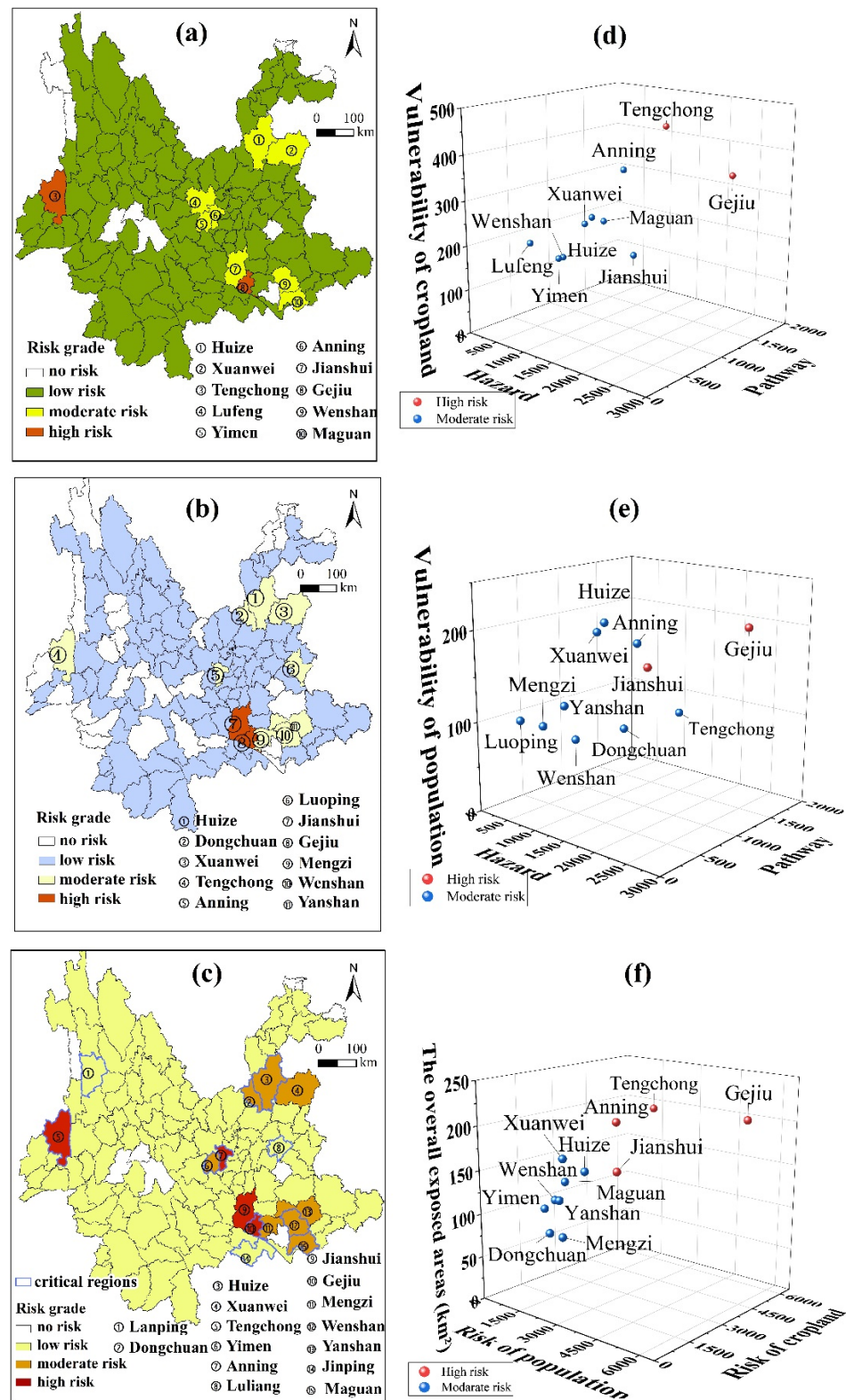


**Figure 8.** Risk assessment at the county scale for (a) cropland, (b) the sensitive population, and (c) the overall risk in Yunnan. The critical regions are outlined in blue in (c) and are recognized as crucial metal pollution regions by the national government. Decomposition of high-risk and moderate-risk regions for (d) croplands, (e) sensitive population, and (f) the overall risk.

In addition, the estimated receptor data, mainly the simulated population data, were verified with statistical data (Figure S1). The main pathway data, including simulated wind and precipitation data, were verified with meteorological station data (Figures S2–S4).

In terms of the verification of the risk assessment, the pollution regions identified by the government were compared. In 2011, the national government reported 11 counties in Yunnan as critically metal-polluted regions, mapped by the blue border in Figure 8c [63]. The 12 at risk counties identified in the current study were compared with those identified by the government. Eight are consistent with the national report, indicating the effectiveness of using multi-source data. Among the three inconsistent counties, Lanping and Jinping counties have high hazard scores, but because of the few receptors in the PHA, their vulnerability scores are low; thus, their overall risk scores are low based on this approach. In addition, Luliang was removed from the list of critically polluted regions in response to restoration efforts in 2015 [64]; therefore, it is not identified in our assessment.

Four counties not listed as critical regions by the national government are identified here as risk regions: Jianshui, Mengzi, Yanshan, and Xuanwei. Both Jianshui and Mengzi counties were included among the key investigated regions during the environmental protection supervision in 2017 in Yunnan [65]. Yanshan was listed as a pilot project for metal pollution prevention in 2016, whereas Xuanwei was estimated to have a very high prevalence of lung cancer (4–8-fold higher than the national average) due to metal pollution [66]. Based on such data, we confirm that multi-source data can reliably be used for regional risk assessment.

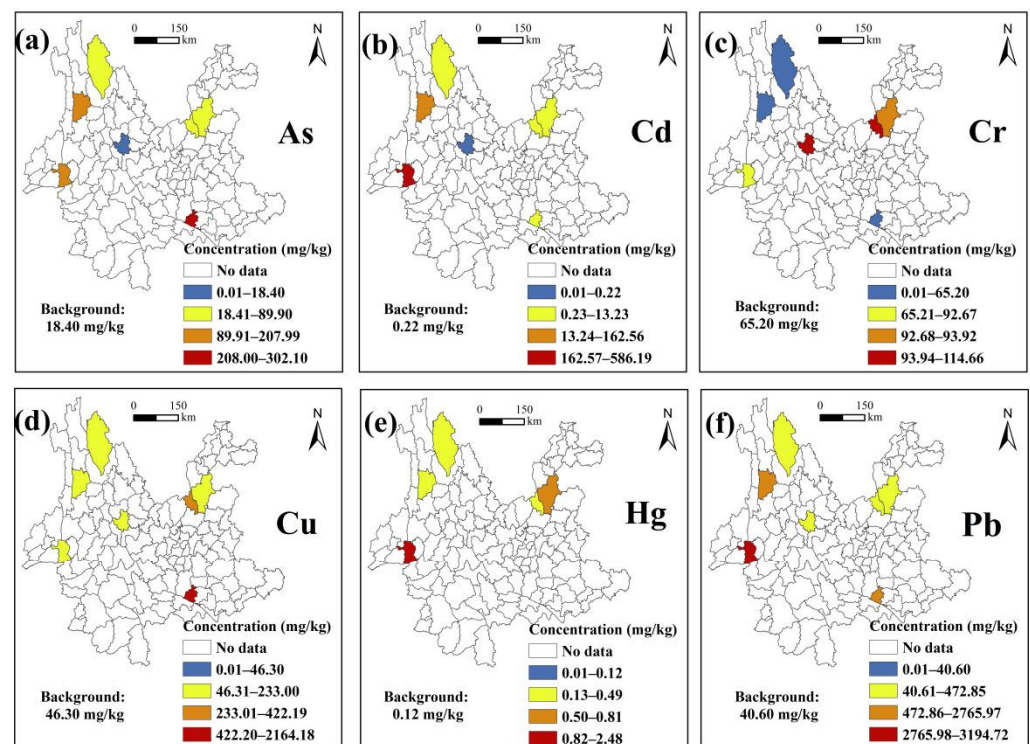
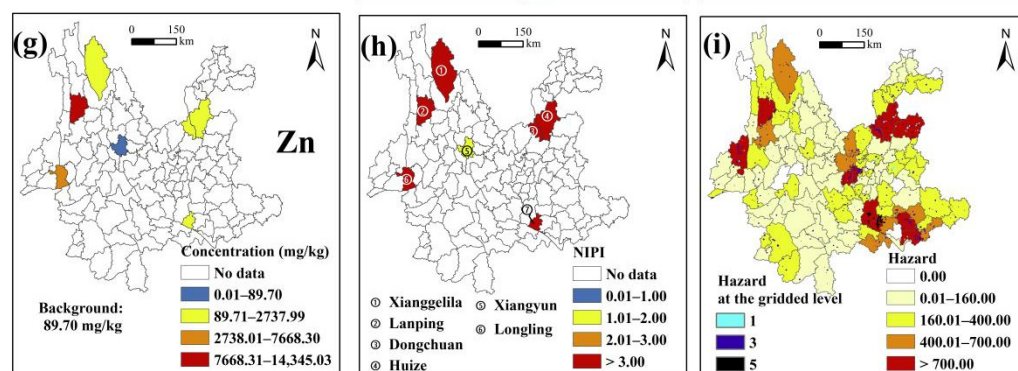


Figure 9. Cont.



**Figure 9.** Verification of the hazard score. Concentrations of heavy metals (a–g). Nemerow integrated pollution index (NIPI) (h). Hazard at the gridded and the county levels (i). The background values of the heavy metals were obtained from Bai, Cui [67].

## 4. Discussion

### 4.1. Contributions

Conducting an accurate regional risk assessment is one of the key prerequisites for developing policies to control pollution [68]. However, the absence of sufficient data often makes that a challenging task. Therefore, previous regional assessments were conducted at a coarse level [17,18]. The current study proposed using multi-source data to overcome this issue, particularly for regions where little or no information is available from site-specific investigations [69]. The verification demonstrates the effectiveness of multi-source data for identifying risks. This is mainly attributed to the multi-source data containing metal-related industrial plants and information about their activities. Great damage to the environment can be caused by PTMs-related activities, especially unsustainable production activities [70,71]. Therefore, the multi-source data involving industrial activity information can provide insight into hazard and risk extents.

Importantly, using multi-source data for large area assessment is cost-effective and efficient when compared with the traditional sampling assessment framework. Hence, it can supplement the sampling assessment method, and plays a significant role in reducing the investigation costs. Furthermore, multi-source data, including internet data and remote sensing images, are flexible data and can, therefore, be adapted to different regions; they are global data and generally free. This means the proposed method can be a useful tool in environmental policy decision-making, and be involved in regional or even global sustainable planning processes, such as the 2030 Agenda for the Sustainable Development Goals (SDGs). The SDG 12 (Sustainable Consumption and Production) requires expanding and accelerating international assessments of chemical risks [72], which coincides with the advantages of the proposed method. In addition, the SDG 3 (Health and Population) regards reducing the number of deaths and illnesses from hazardous chemicals and pollution as one of its associated targets [73], which also can be supported by the proposed method.

One of the key contributions of multi-source data to the assessments is to provide gridded information. Regional assessments target the identification and screening of actual or suspected contaminated sites needing further actions (such as investigation or remediation). The grid-scale assessed results thereby represent a more precise guide for further investigation than the administrative-scale results [74,75].

The novel PHA simulation model developed here estimates the potential contaminated zone based on the factors associated with industrial plant production and the natural environment. Unlike in previous studies, a special potential risk area was simulated for each industrial plant, thereby resolving the challenges of an oversimplified approach [10,76].

#### 4.2. Management Suggestions

According to the dominant risk component, the 12 high- and moderate-risk counties can be grouped into four types: comprehensive, cropland-vulnerable, population-vulnerable, and ordinary. The management proposals for each type are listed in Table 4. In general, to optimize that the spatial layout, high-hazard plants in close vicinity to cropland-intensive and densely populated areas should be either closed or moved to low-risk regions. Furthermore, where prevailing winds are significant, industrial plants should be established or relocated downwind of residential areas or cropland.

**Table 4.** Counties associated with different types of risk and the proposed management strategies.

Risk Types	Counties	Management Strategies
Comprehensive	Gejiu, Anning	(1) Strengthen supervision of potential polluting factories with probable pollutants, and shut down or remove factories with excessive pollution; (2) Adjust the industrial structure and reduce the proportion of industries involved in pollution; (3) Optimize the spatial layout and isolate the potential polluting factories from cropland-intensive and densely populated areas by distance or barriers.
Cropland-vulnerable	Tengchong, Maguan	(1) Intensify the supervision of the discharge of existing potential polluting factories to cropland, and shut down or relocate them when necessary; (2) Optimize the spatial distribution of industries and keep the potential polluting factories away from cropland-intensive areas, especially those with high yields; (3) Cultivate low-accumulation crops or purchase food from low-risk regions.
Population-vulnerable	Jianshui, Huize	(1) Strengthen the supervision of potential polluting factories, and shut down or relocate them when necessary; (2) Optimize the spatial distribution and keep the potential polluting factories away from densely populated areas.
Ordinary	Xuanwei, Mengzi, Yanshan, Wenshan, Dongchuan, Yimen	(1) Strengthen the supervision of potential polluting factories and reorganize or shut down factories with excessive pollution; (2) Upgrade the market access threshold for factories and prohibit the expansion of high-risk pollution-associated factories.

#### 4.3. Limitations

Although the proposed approach achieves a desirable outcome, there are some uncertainties that should be noted. First, bias was expected if there were omissions in the mining data set. Industrial plants in China need to register for national government organizations, such as the State Administration for Market Regulation, before operation, which enables the government organizations to collect almost all industrial plant information across the country. The two main internet platforms we used, TianYanCha and GNEDC, have collected information from government organizations on at least 280 million industrial plants across China, capturing the majority of the sources of interest. However, for countries and regions other than China, a pre-assessment of their mining data sets is strongly recommended. In addition, there is a bias in that some small unregistered industrial plants were not included, and this bias is also involved in national supervision. To address this issue, an application of remote sensing images for identifying industrial plants and their emission activities is recommended in future studies.

Ideally, the hazard of an industrial plant would be expressed in terms of its production, volumes of produced waste, and toxicity characterization of released pollutants, among others [10]. However, due to data limitations, the industrial index, the duration of operation, and the kernel density (Equation (1)) were used to quantify the hazard in the current paper. Despite this limitation, the industrial index was evaluated based on factory pollution infractions and was, therefore, somewhat representative of the hazard posed by each infraction. Nevertheless, with the support of additional investigations, the assessment is amenable to refinement.

Although atmospheric deposition is the predominant pathway of PTMs contamination [77,78], waterbodies, as important exposure sources and potential exposure pathways [10], should also be considered as main pathways and receptors, whenever relevant data are available. In addition, subgroups of sensitive populations, such as children, elderly individuals, and immunocompromised individuals, may respond differently to PTMs pollution [79]. For example, children are more likely to face non-carcinogenic risks due to heavy metal pollution than elderly people [33]. Therefore, a stratification analysis is expected to improve the assessment methodology. Nevertheless, the primary objective here was to evaluate the effectiveness of multi-source data in regional risk assessment, and stratified sensitive populations can be considered when such data are available.

Whilst the verification was conducted by comparing our results to government reports and previous publications, a field point-level verification was lacking. The regional assessment aimed at the prescreening of high-potential pollution zones before conducting any point-level investigation. Therefore, we believe that cross-checking with government reports and previous publications was a reasonable approach to verifying the reliability of the results.

## 5. Conclusions

The difficulty in obtaining data is a primary impediment of regional risk assessment. In this study, we proposed using multi-source data for regional risk assessment of PTMs, and conducted a case study in Yunnan Province. The assessed results indicate that the risk areas are mostly concentrated in the eastern province, with 3.6% of the cropland and 1.4% of the sensitive population suffering from contamination threats. At the county level, there are 12 high- and moderate-risk counties, including Gejiu, which currently faces the greatest risk. Furthermore, verification confirms the reliability of multi-source data. This suggests that multi-source data can complement environmental field sampling to some extent, which make sense when assessing remote large areas, given the large amounts of resources usually involved in conducting (and maintaining) field collections. In addition, except PTMs, multi-source data and the potentially hazardous area simulation developed here are also applicable to expose other environmental contaminants.

**Supplementary Materials:** The following supporting information can be downloaded at: <https://www.mdpi.com/article/10.3390/ijgi11080427/s1>, Figure S1: Scatter plot between total estimated population and total population based on the 2015 census at the prefectural level; Figure S2: Distribution of meteorological stations; Figure S3: Scatter plot between simulated wind speed and stations wind speed; Figure S4: Scatter plot between simulated precipitation and stations precipitation; Table S1: The statistical information of the crawled industrial plants; Table S2: The assessed results of high and moderate risk-counties in Yunnan Province; Table S3: List of the literature used in this study.

**Author Contributions:** Study conception and design, Hongyan Cai and Mulin Chen; data collection, Mei Lei and Mulin Chen; analysis and interpretation of results, Mulin Chen; draft manuscript preparation, Hongyan Cai, Mulin Chen, Li Wang, and Mei Lei. All authors have read and agreed to the published version of the manuscript.

**Funding:** This work was supported by the National Key R&D Program of China [NO. 2018YFC1800103].

**Institutional Review Board Statement:** Not applicable.

**Informed Consent Statement:** Not applicable.

**Data Availability Statement:** Not applicable.

**Acknowledgments:** We are thankful to the anonymous reviewers and handling editors for their constructive comments in improving this manuscript.

**Conflicts of Interest:** The authors declare no conflict of interest.

## References

1. Rahman, M.; Khan, M.; Jolly, Y.; Kabir, J.; Akter, S.; Salam, A. Assessing risk to human health for heavy metal contamination through street dust in the Southeast Asian Megacity: Dhaka, Bangladesh. *Sci. Total Environ.* **2019**, *660*, 1610–1622. [[CrossRef](#)] [[PubMed](#)]
2. Weidenhamer, J.; Fitzpatrick, M.; Biro, A.; Kobunski, P.; Hudson, M.; Corbin, R.; Gottesfeld, P. Metal exposures from aluminum cookware: An unrecognized public health risk in developing countries. *Sci. Total Environ.* **2017**, *579*, 805–813. [[PubMed](#)]
3. Li, F.; Zhang, J.; Yang, J.; Liu, C.; Zeng, G. Site-specific risk assessment and integrated management decision-making: A case study of a typical heavy metal contaminated site, Middle China. *Hum. Ecol. Risk Assess.* **2016**, *22*, 1224–1241. [[CrossRef](#)]
4. Li, F.; Zhang, J.; Jiang, W.; Liu, C.; Zhang, Z.; Zhang, C.; Zeng, G. Spatial health risk assessment and hierarchical risk management for mercury in soils from a typical contaminated site, China. *Environ. Geochem. Health* **2017**, *39*, 923–934.
5. Shao, D.; Zhan, Y.; Zhou, W.; Zhu, L. Current status and temporal trend of heavy metals in farmland soil of the Yangtze River Delta Region: Field survey and meta-analysis. *Environ. Pollut.* **2016**, *219*, 329–336. [[CrossRef](#)]
6. Tóth, G.; Hermann, T.; Szatmári, G.; Pásztor, L. Maps of heavy metals in the soils of the European Union and proposed priority areas for detailed assessment. *Sci. Total Environ.* **2016**, *565*, 1054–1062.
7. Desaulles, A. Critical evaluation of soil contamination assessment methods for trace metals. *Sci. Total Environ.* **2012**, *426*, 120–131. [[CrossRef](#)]
8. Li, R.; Yuan, Y.; Li, C.; Sun, W.; Yang, M.; Wang, X. Environmental health and ecological risk assessment of soil heavy metal pollution in the coastal cities of Estuarine Bay—A case study of Hangzhou Bay, China. *Toxics* **2020**, *8*, 75.
9. Kielenniva, N.; Antikainen, R.; Sorvari, J. Measuring eco-efficiency of contaminated soil management at the regional level. *J. Environ. Manag.* **2012**, *109*, 179–188. [[CrossRef](#)]
10. Pizzol, L.; Critto, A.; Agostini, P.; Marcomini, A. Regional risk assessment for contaminated sites part 2: Ranking of potentially contaminated sites. *Environ. Int.* **2011**, *37*, 1307–1320.
11. Li, D.; Zhang, C.; Pizzol, L.; Critto, A.; Zhang, H.; Lv, S.; Marcomini, A. Regional risk assessment approaches to land planning for industrial polluted areas in China: The Hulunbeier region case study. *Environ. Int.* **2014**, *65*, 16–32. [[CrossRef](#)]
12. Henny, C.; Meutia, A. Urban lakes in megacity Jakarta: Risk and management plan for future sustainability. *Procedia Environ. Sci.* **2014**, *20*, 737–746. [[CrossRef](#)]
13. Minolfi, G.; Albanese, S.; Lima, A.; Tarvainen, T.; Fortelli, A.; De, V. A regional approach to the environmental risk assessment—Human health risk assessment case study in the Campania region. *J. Geochem. Explor.* **2018**, *184*, 400–416. [[CrossRef](#)]
14. Petrik, A.; Thiombane, M.; Albanese, S.; Lima, A.; De, V. Source patterns of Zn, Pb, Cr and Ni potentially toxic elements (PTEs) through a compositional discrimination analysis: A case study on the Campanian topsoil data. *Geoderma* **2018**, *331*, 87–99. [[CrossRef](#)]
15. Zuzolo, D.; Cichella, D.; Lima, A.; Guagliardi, I.; Cerino, P.; Pizzolante, A.; Thiombane, M.; De, V.; Albanese, S. Potentially toxic elements in soils of Campania region (Southern Italy): Combining raw and compositional data. *J. Geochem. Explor.* **2020**, *213*, 106524. [[CrossRef](#)]
16. Agostini, P.; Pizzol, L.; Critto, A.; D'Alessandro, M.; Zabeo, A.; Marcomini, A. Regional risk assessment for contaminated sites part 3: Spatial decision support system. *Environ. Int.* **2012**, *48*, 121–132. [[CrossRef](#)]
17. Huang, Y.; Wang, L.; Wang, W.; Li, T.; He, Z.; Yang, X. Current status of agricultural soil pollution by heavy metals in China: A meta-analysis. *Sci. Total Environ.* **2019**, *651*, 3034–3042. [[CrossRef](#)]
18. Pan, L.; Wang, Y.; Ma, J.; Hu, Y.; Su, B.; Fang, G.; Wang, L.; Xiang, B. A review of heavy metal pollution levels and health risk assessment of urban soils in Chinese cities. *Environ. Sci. Pollut. Res.* **2018**, *25*, 1055–1069. [[CrossRef](#)]
19. Hou, S.; Zheng, N.; Tang, L.; Ji, X.; Li, Y.; Hua, X. Pollution characteristics, sources, and health risk assessment of human exposure to Cu, Zn, Cd and Pb pollution in urban street dust across China between 2009 and 2018. *Environ. Int.* **2019**, *128*, 430–437. [[CrossRef](#)]
20. Sun, M.; Wang, T.; Xu, X.; Zhang, L.; Li, J.; Shi, Y. Ecological risk assessment of soil cadmium in China's coastal economic development zone: A meta-analysis. *Ecosyst. Health Sustain.* **2020**, *6*, 1733921. [[CrossRef](#)]
21. Yang, Q.; Li, Z.; Lu, X.; Duan, Q.; Huang, L.; Bi, J. A review of soil heavy metal pollution from industrial and agricultural regions in China: Pollution and risk assessment. *Sci. Total Environ.* **2018**, *642*, 690–700. [[CrossRef](#)]
22. Zhang, X.; Zha, T.; Guo, X.; Meng, G.; Zhou, J. Spatial distribution of metal pollution of soils of Chinese provincial capital cities. *Sci. Total Environ.* **2018**, *643*, 1502–1513. [[CrossRef](#)]
23. Hu, B.; Shao, S.; Ni, H.; Fu, Z.; Hu, L.; Zhou, Y.; Min, X.; She, S.; Chen, S.; Huang, M.; et al. Current status, spatial features, health risks, and potential driving factors of soil heavy metal pollution in China at province level. *Environ. Pollut.* **2020**, *266*, 114961. [[CrossRef](#)]
24. Teng, Y.; Ni, S.; Wang, J.; Zuo, R.; Yang, J. A geochemical survey of trace elements in agricultural and non-agricultural topsoil in Dexing area, China. *J. Geochem. Explor.* **2010**, *104*, 118–127. [[CrossRef](#)]
25. Werner, T.; Bebbington, A.; Gregory, G. Assessing impacts of mining: Recent contributions from GIS and remote sensing. *Extr. Ind. Soc.* **2019**, *6*, 993–1012. [[CrossRef](#)]
26. Saedpanah, S.; Amanollahi, J. Environmental pollution and geo-ecological risk assessment of the Qhorveh mining area in western Iran. *Environ. Pollut.* **2019**, *253*, 811–820. [[CrossRef](#)]

27. Zhong, Y.; Wang, X.; Xu, Y.; Wang, S.; Jia, T.; Hu, X.; Zhao, J.; Wei, L.; Zhang, L. Mini-UAV-borne hyperspectral remote sensing: From observation and processing to applications. *IEEE Geosci. Remote Sens. Mag.* **2018**, *6*, 46–62. [[CrossRef](#)]
28. Song, Y.; Huang, B.; Cai, J.; Chen, B. Dynamic assessments of population exposure to urban greenspace using multi-source big data. *Sci. Total Environ.* **2018**, *634*, 1315–1325. [[CrossRef](#)]
29. Li, Y.; He, D.; Hu, J.; Cao, J. Variability of extreme precipitation over Yunnan Province, China 1960–2012. *Int. J. Climatol.* **2015**, *35*, 245–258. [[CrossRef](#)]
30. Lu, L.; Cheng, H.; Liu, X.; Xie, J.; Li, Q.; Zhou, T. Assessment of regional human health risks from lead contamination in Yunnan province, southwestern China. *PLoS ONE* **2015**, *10*, e0119562. [[CrossRef](#)]
31. Pu, W.; Sun, J.; Zhang, F.; Wen, X.; Liu, W.; Huang, C. Effects of copper mining on heavy metal contamination in a rice agrosystem in the Xiaojiang River Basin, southwest China. *Acta Geochim.* **2019**, *38*, 753–773. [[CrossRef](#)]
32. Chen, H.; Teng, Y.; Lu, S.; Wang, Y.; Wang, J. Contamination features and health risk of soil heavy metals in China. *Sci. Total Environ.* **2015**, *512*, 143–153. [[CrossRef](#)] [[PubMed](#)]
33. Fan, Y.; Jiang, Y.; Chang, R.; Yao, S.; Jin, P.; Wang, W.; He, J.; Zhou, Q.; Prorok, P.; Qiao, Y.; et al. Prior lung disease and lung cancer risk in an occupational-based cohort in Yunnan, China. *Lung Cancer* **2011**, *72*, 258–263. [[CrossRef](#)] [[PubMed](#)]
34. GNEDC. *Guidelines for the Evaluation of Enterprise Environmental Risk Index*; GNEDC: Guangzhou, China, 2018.
35. Xiao, C.; Feng, Z.; Li, P.; You, Z.; Teng, J. Evaluating the suitability of different terrains for sustaining human settlements according to the local elevation range in China using the ASTER GDEM. *J. Mt. Sci.* **2018**, *15*, 2741–2751. [[CrossRef](#)]
36. MEE. Notice on the Issuance of a Series of Technical Guidelines for Site Survey of Key Enterprises. Available online: [http://www.mee.gov.cn/gkml/hbb/bgt/201708/t20170818\\_420021.htm](http://www.mee.gov.cn/gkml/hbb/bgt/201708/t20170818_420021.htm) (accessed on 14 August 2018).
37. MEE. Technical Guidelines for Risk Assessment of Soil Contamination of Land for Construction (HJ 25.3-2019). Available online: [https://www.mee.gov.cn/ywgz/fgbz/bz/bzwb/trhj/201912/t20191224\\_749893.shtml](https://www.mee.gov.cn/ywgz/fgbz/bz/bzwb/trhj/201912/t20191224_749893.shtml) (accessed on 5 December 2019).
38. Lu, D.; Weng, Q.; Li, G. Residential population estimation using a remote sensing derived impervious surface approach. *Int. J. Remote Sens.* **2006**, *27*, 3553–3570. [[CrossRef](#)]
39. Lobell, D.; Hicke, J.; Asner, G.; Field, C.; Tucker, C.; Los, S. Satellite estimates of productivity and light use efficiency in United States agriculture, 1982–98. *Glob. Change Biol.* **2002**, *8*, 722–735. [[CrossRef](#)]
40. He, B.; Zhao, X.; Li, P.; Liang, J.; Fan, Q.; Ma, X.; Zheng, G.; Qiu, J. Lead isotopic fingerprinting as a tracer to identify the pollution sources of heavy metals in the southeastern zone of Baiyin, China. *Sci. Total Environ.* **2019**, *660*, 348–357. [[CrossRef](#)]
41. Wang, Q.; Hao, D.; Wang, F.; Wang, H.; Huang, X.; Li, F.; Li, C.; Yu, H. Development of a new framework to estimate the environmental risk of heavy metal (loid) s focusing on the spatial heterogeneity of the industrial layout. *Environ. Int.* **2021**, *147*, 106315. [[CrossRef](#)]
42. MEE. Technical Provisions for the Detailed Investigation of Soil Pollution in Agricultural land. Available online: [https://www.sohu.com/a/403023950\\_100051699](https://www.sohu.com/a/403023950_100051699) (accessed on 21 May 2019).
43. Punia, A. Role of temperature, wind, and precipitation in heavy metal contamination at copper mines: A review. *Environ. Sci. Pollut. Res.* **2020**, 1–17. [[CrossRef](#)]
44. Fry, K.; Gillings, M.; Isley, C.; Gunkel-Grillon, P.; Taylor, M. Trace element contamination of soil and dust by a New Caledonian ferronickel smelter: Dispersal, enrichment, and human health risk. *Environ. Pollut.* **2021**, *288*, 117593. [[CrossRef](#)]
45. Colgan, A.; Hankard, P.; Spurgeon, D.; Svendsen, C.; Wadsworth, R.; Weeks, J. Closing the loop: A spatial analysis to link observed environmental damage to predicted heavy metal emissions. *Environ. Toxicol. Chem.* **2003**, *22*, 970–976. [[CrossRef](#)]
46. Al-Khashman, O.; Shawabkeh, R. Metals distribution in soils around the cement factory in southern Jordan. *Environ. Pollut.* **2006**, *140*, 387–394. [[CrossRef](#)]
47. Dragović, R.; Gajić, B.; Dragović, S.; Đorđević, M.; Đorđević, M.; Mihailović, N.; Onjia, A. Assessment of the impact of geographical factors on the spatial distribution of heavy metals in soils around the steel production facility in Smederevo (Serbia). *J. Clean. Prod.* **2014**, *84*, 550–562. [[CrossRef](#)]
48. Filimonova, L.; Parshin, A.; Bychinskii, V. Air pollution assessment in the area of aluminum production by snow geochemical survey. *Russ. Meteorol. Hydrol.* **2015**, *40*, 691–698. [[CrossRef](#)]
49. Li, R.; Li, Q.; Chen, S.; Wu, F.; Sun, D.; Liao, H. Distribution of thorium in soils surrounding the rare-earth tailings reservoir in Baotou, China. *J. Radioanal. Nucl. Chem.* **2014**, *299*, 1453–1459. [[CrossRef](#)]
50. Ooms, G.; Mahieu, A. A comparison between a plume path model and a virtual point source model for a stack plume. *Appl. Sci. Res.* **1981**, *36*, 339–356. [[CrossRef](#)]
51. Fouda, Y. A GIS for environmental assessment of air pollution impacts on urban clusters and natural landscape at Rosetta City and region, Egypt. *Urban Ecosyst.* **2001**, *5*, 5–25. [[CrossRef](#)]
52. Hou, D.; O'Connor, D.; Nathanail, P.; Tian, L.; Ma, Y. Integrated GIS and multivariate statistical analysis for regional scale assessment of heavy metal soil contamination: A critical review. *Environ. Pollut.* **2017**, *231*, 1188–1200. [[CrossRef](#)]
53. Hui, Y.; Yong, L.; Shaoquan, L.; Yong, W.; Yong, Y.; Weidong, L. The influences of topographic relief on spatial distribution of mountain settlements in Three Gorges Area. *Environ. Earth Sci.* **2015**, *74*, 4335–4344. [[CrossRef](#)]
54. Shi, Y.; Zhao, J.; Li, C. Spatial-temporal distribution characteristics of farmland ecosystem productivity of typical oasis in Zhangye City. *Bull. Soil Water Conserv.* **2017**, *37*, 120–125.
55. Greenmine. 2016. Available online: [http://www.greenmine.org.cn/upload/grab/20160929/81148233\\_31.png](http://www.greenmine.org.cn/upload/grab/20160929/81148233_31.png) (accessed on 23 April 2019).



56. Guo, Y. Analysis of spatio-temporal changes in life expectancy and its influencing factors in China. *Chin. J. Health Policy* **2018**, *11*, 44–49.
57. Wei, M.; Su, Z.; Wang, J.; Gonzalez, M.; Yu, X.; Liang, H.; Zhou, Q.; Fan, Y.; Qiao, Y. Performance of lung cancer screening with low-dose CT in Gejiu, Yunnan: A population-based, screening cohort study. *Thorac. Cancer* **2020**, *11*, 1224–1232. [[CrossRef](#)]
58. Qiao, Y.; Taylor, P.; Yao, S.; Erozan, Y.; Luo, X.; Barrett, M.; Yan, Q.; Giffen, C.; Huang, S.; Maher, M.; et al. Risk factors and early detection of lung cancer in a cohort of Chinese tin miners. *Ann. Epidemiol.* **1997**, *7*, 533–541. [[CrossRef](#)]
59. Fan, Y.; Liang, H.; Qiao, Y. Lung cancer in urban China. *Cancer Control* **2015**, *7*, 88–93.
60. Li, P.; Lin, C.; Cheng, H.; Duan, X.; Lei, K. Contamination and health risks of soil heavy metals around a lead/zinc smelter in southwestern China. *Ecotoxicol. Environ. Saf.* **2015**, *113*, 391–399. [[CrossRef](#)]
61. Yang, J.; Yang, F.; Yang, Y.; Xing, G.; Deng, C.; Shen, Y.; Luo, L.; Li, B.; Yuan, H. A proposal of “core enzyme” bioindicator in long-term Pb-Zn ore pollution areas based on topsoil property analysis. *Environ. Pollut.* **2016**, *213*, 760–769. [[CrossRef](#)]
62. Cheng, H.; Li, M.; Zhao, C.; Li, K.; Peng, M.; Qin, A.; Cheng, X. Overview of trace metals in the urban soil of 31 metropolises in China. *J. Geochem. Explor.* **2014**, *139*, 31–52. [[CrossRef](#)]
63. MEE. Heavy Metal Pollution Prevention Deployment in Yunnan Province. Available online: [http://www.mee.gov.cn/ywdt/hjnews/201105/t20110520\\_210913.shtml](http://www.mee.gov.cn/ywdt/hjnews/201105/t20110520_210913.shtml) (accessed on 16 May 2019).
64. Wang, H. Measures and effects of heavy metal pollution control in Luliang County. *Environ. Sci. Surv.* **2017**, *36*, 139–142.
65. Environmental Protection and Remediation Plan of Honghe City. Available online: [http://sthjt.yn.gov.cn/ywdt/xxywrdjj/201907/t20190730\\_191420.html](http://sthjt.yn.gov.cn/ywdt/xxywrdjj/201907/t20190730_191420.html) (accessed on 26 April 2019).
66. Tan, Z.; Lu, S.; Zhao, H.; Kai, X.; Jiexian, P.; Win, M.; Yu, S.; Yonemochi, S.; Wang, Q. Magnetic, geochemical characterization and health risk assessment of road dust in Xuanwei and Fuyuan, China. *Environ. Geochem. Health* **2018**, *40*, 1541–1555. [[CrossRef](#)]
67. Bai, J.; Cui, B.; Wang, Q.; Gao, H.; Ding, Q. Assessment of heavy metal contamination of roadside soils in Southwest China. *Stoch. Environ. Res. Risk Assess.* **2009**, *23*, 341–347. [[CrossRef](#)]
68. Xiang, M.; Li, Y.; Yang, J.; Li, Y.; Li, F.; Hu, B.; Cao, Y. Assessment of heavy metal pollution in soil and classification of pollution risk management and control zones in the industrial developed city. *Environ. Manag.* **2020**, *66*, 1105–1119. [[CrossRef](#)] [[PubMed](#)]
69. Qu, C.; De, V.; Albanese, S.; Fortelli, A.; Scafetta, N.; Li, J.; Hope, D.; Cerino, P.; Pizzolante, A.; Qi, S.; et al. High spatial resolution measurements of passive-sampler derived air concentrations of persistent organic pollutants in the Campania region, Italy: Implications for source identification and risk analysis. *Environ. Pollut.* **2021**, *286*, 117248. [[CrossRef](#)] [[PubMed](#)]
70. Marove, C.; Sotozono, R.; Tangviroon, P.; Tabelin, C.; Igarashi, T. Assessment of soil, sediment and water contaminations around open-pit coal mines in Moatize, Tete province, Mozambique. *Environ. Adv.* **2022**, *8*, 100215. [[CrossRef](#)]
71. Iordanidis, A.; Zoras, S.; Triantafyllou, A.; Buckman, J.; Asvesta, A.; Evagelopoulos, V. Characterisation of airborne particles collected proximal to lignite mines and power plants of Ptolemais-Kozani area, northern Greece. *Fresenius Environ. Bull.* **2008**, *17*, 378–398.
72. Gasper, D.; Shah, A.; Tankha, S. The framing of sustainable consumption and production in SDG 12. *Glob. Policy* **2019**, *10*, 83–95. [[CrossRef](#)]
73. Asi, Y.; Williams, C. The role of digital health in making progress toward Sustainable Development Goal (SDG) 3 in conflict-affected populations. *Int. J. Med. Inform.* **2018**, *114*, 114–120. [[CrossRef](#)]
74. Tsakmakis, I.; Kokkos, N.; Pisinaras, V.; Papaevangelou, V.; Hatzigiannakis, E.; Arampatzis, G.; Gikas, G.; Linker, R.; Zoras, S.; Evagelopoulos, V.; et al. Operational precise irrigation for cotton cultivation through the coupling of meteorological and crop growth models. *Water Resour. Manag.* **2017**, *31*, 563–580. [[CrossRef](#)]
75. Zoras, S.; Triantafyllou, A.; Hurley, P. Grid sensitivity analysis for the calibration of a prognostic meteorological model in complex terrain by a screening experiment. *Environ. Model. Softw.* **2007**, *22*, 33–39. [[CrossRef](#)]
76. Wang, Q.; Liu, J.; Chen, Z.; Li, F.; Yu, H. A causation-based method developed for an integrated risk assessment of heavy metals in soil. *Sci. Total Environ.* **2018**, *642*, 1396–1405. [[CrossRef](#)]
77. Deng, W.; Li, X.; An, Z.; Yang, L. The occurrence and sources of heavy metal contamination in peri-urban and smelting contaminated sites in Baoji, China. *Environ. Monit. Assess.* **2016**, *188*, 251. [[CrossRef](#)]
78. Shi, T.; Ma, J.; Wu, X.; Ju, T.; Lin, X.; Zhang, Y.; Li, X.; Gong, Y.; Hou, H.; Zhao, L.; et al. Inventories of heavy metal inputs and outputs to and from agricultural soils: A review. *Ecotoxicol. Environ. Saf.* **2018**, *164*, 118–124. [[CrossRef](#)]
79. Islam, M.; Das, B.; Huque, M. Risk assessment for bangladeshis due to arsenic exposure from consumption of vegetables grown with natural arsenic contaminated groundwater. *Indian J. Sci. Technol.* **2018**, *11*, 5645. [[CrossRef](#)]